JOURNAL OF MAGNETIC RESONANCE **125,** 212–215 (1997)
ARTICLE NO. MN971115

Field Stabilization and ^{2}H NMR Spectroscopy in a 24.6 T Resistive Magnet

V. SOGHOMONIAN, M. COTTEN, R. ROSANSKE, AND T. A. CROSS

Center for Interdisciplinary Magnetic Resonance at the National High Magnetic Field Laboratory, Institute of Molecular Biophysics, and Department of Chemistry, Florida State University, Tallahassee, Florida 32306-4005

Received December 12, 1996

The NHMFL has installed a 24.6 T (~1 GHz ^{1}H) resistive magnet with improved homogeneity to explore possibilities for NMR spectroscopy at field strengths higher than those obtained in current superconducting magnets. Here, a characterization of this magnet is presented along with a discussion of spectroscopic implications and the first-phase technical solutions. In addition, ^{2}H NMR spectra of powders and oriented samples demonstrate some advantages and disadvantages in working at very high magnetic fields.

Currently, the highest magnetic fields available in superconducting magnets are less than 21 T (900 MHz for ^{1}H). Resistive magnets offer higher field strengths at the expense of temporal stability and field homogeneity. In this paper, we present these temporal and spatial homogeneity problems that are associated with the 24.6 T resistive magnet installed at the NHMFL (*1*) and present the first phase corrections that permit moderate-resolution solid-state NMR spectroscopy.

Literature abounds (*2–5*) on the advantages and disadvantages of high magnetic fields for NMR spectroscopy. The advantages include enhanced sensitivity and resolution, reduction in second-order effects such as those between Zeeman and quadrupole interactions, changes in the relaxation properties, and increased chemical-shift dispersion, among others. In the 24.6 T magnet system, two advantages of high B_0 fields are demonstrated for solid-state ^{2}H spectra: (1) reduction of tau values in quadrupole echo sequences that allows for the detection of spin sites possessing short relaxation times and (2) enhanced sensitivity.

Figure 1 shows a cross section of the magnet, which consists of three concentric stacks of Bitter disks of height 470 mm and diameter 610 mm, contained in a stainless steel housing. The magnet is located in a bay that affords two 10 MW power supplies and a cooling water loop. There are two current leads attached to the magnet, providing a maximum total of 40 kA. This particular magnet consumes, at full field, 12.6 MW at 35.5 kA. Under these conditions, deionized cooling water is cycled through the magnet at the rate of 4500 L/min at a pressure of 2 MPa (300 psi). Cooling water enters the magnet from the top with an inlet temperature of 8°C and exits the magnet from the bottom with a temperature of around 35°C. Each current lead has current-carrying capability according to MCM 3000 (equivalent to a copper rod 44 mm in diameter) and is jacketed by circulating water to prevent overheating. The current leads, water pipes, and magnet are placed under a platform that is utilized by experimenters to gain top loading access to the magnet. The magnet rests on legs that position the bottom plate 920 mm from the ground, ensuring access to the bore from below. The magnet center is 587 mm from the top flange, and the experimentally available bore is 32.0 mm in diameter. The bore tube is circumscribed by the water-cooled stacks of perforated copper plates or Bitter disks, which are connected in series. To increase the homogenous volume and to improve the *Z*-axis spatial homogeneity of this magnet, a 52 mm section at the center of coil B (Fig. 1) was electrically shorted (*1*).

The power supply and cooling-water temperature influence the temporal stability of the magnet. A 1°C increase in the inlet water temperature causes a 17 ppm decrease in the magnetic field strength due to a change in magnet efficiency. The power supply has a noise level of 10 ppm manifested as 60 Hz noise and its harmonics, plus some high-frequency noise, e.g., 1440 Hz, presumed to be rectifier switching noise. Under normal operating conditions, the inlet water temperature varies by less than 0.4°C if no other magnet is ramping. The total temporal instability under these conditions is on the order of 16 ppm as shown in Fig. 2A. In the same figure, a strong correlation between the inlet water temperature and the ^{2}H resonance frequency (D_2O in a 2 mm sphere) is demonstrated. The temporal fluctuations display a 2 min oscillatory behavior, which mimics the water temperature control feedback system when operating in auto mode. Placing the water temperature control system in manual mode greatly diminishes this periodicity (data not shown).

To compensate for the temporal instability, a field/frequency lock unit and a flux stabilizer have been installed. The former corrects for low-frequency drift (<5 Hz) caused by cooling water and other factors, while the latter corrects for high-frequency fluctuations caused by the power supply

1090-7807/97 $25.00

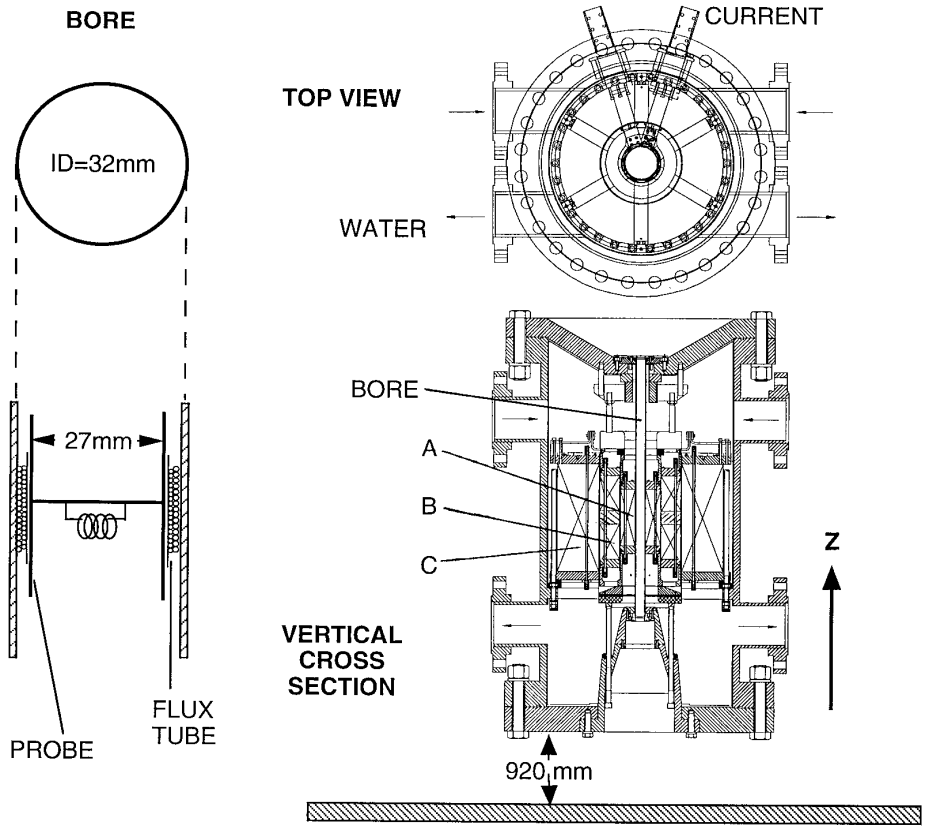

FIG. 1. Top and vertical cross-section views of the magnet depicting the three coils, A, B, and C. The electrically shorted portion of the middle coil (B) is given by the shaded area. The enlargement on the left shows the clear bore diameter (32 mm) and the available space left for the probe after the insertion of the flux stabilizer.

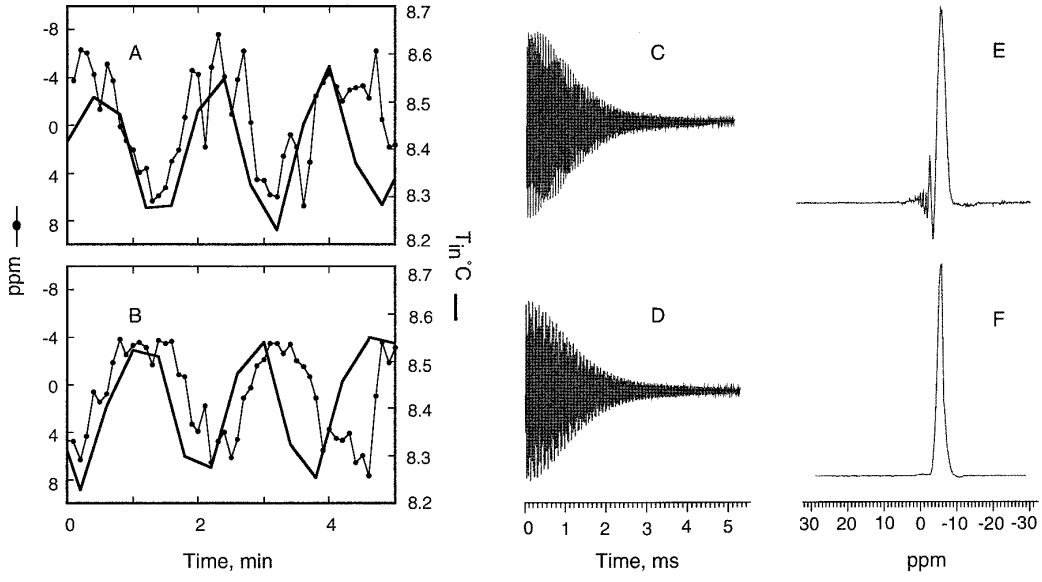

FIG. 2. Temperature of the inlet water and power supply ripple affect the temporal instability of the 24.6 T magnet. (A) Temporal instability without flux stabilization. The heavy line is the temperature trace, whereas the circles represent the ^2H (D_2O) resonance offset frequency at 158 MHz. The field instability without correction is on the order of 16 ppm. (B) As in (A) but with the flux stabilization. Field instability is reduced to 12 ppm. (C, D) The ^2H FIDs without and with flux stabilization, respectively. (E, F) The FT spectra corresponding to (C, D), respectively.

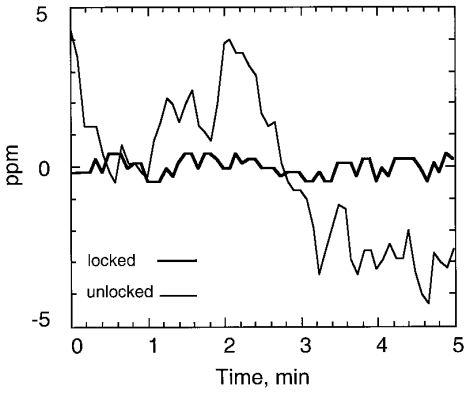

FIG. 3. Effectiveness of a ^{2}H field/frequency lock unit to compensate for slow (<5 Hz) changes in B_0. The resonance frequency of ^{23}Na (aqueous $NaNO_3$) is monitored as a function of time when the magnetic field is unlocked (thinner line) and when it is locked (heavy line). A temporal stability of 0.9 ppm is achieved when the field is locked.

(5–1500 Hz). The flux stabilizer consists of pick-up and compensating coils wound as solenoids with their axial direction parallel to the magnetic field. The pick-up coil detects dB_0/dt and compensates for this change by supplying a proportional correction current through the compensating coil. With this flux stabilizer in place, the temporal instability is reduced to 12 ppm, as demonstrated in Fig. 2B. The flux stabilizer virtually eliminates the ''ringing'' shown in Figs. 2E and 2F, and somewhat reduces the linewidth of the D_2O resonance. Without the stabilizer, the field fluctuations generate the appearance of a field or frequency swept resonance as in continuous wave spectrometers. The flux stabilizer results in the more familiar appearance of an FT spectrum (Fig. 2F).

In order to signal average and maintain the resolution shown in Fig. 2F, a field/frequency lock was developed. A continuous train of pulses, every 200 ms, was applied 300 Hz off the resonant frequency of ^{2}H. The free-induction decay was sampled 300 μs after the pulse and placed in a sample and hold circuit. The DC voltage of this circuit was used as the error signal for the lock. This arrangement provided a capture range of 160–180 Hz. The correction signal from the field/frequency lock was summed with that of the flux pickup and fed through the correction coil of the flux stabilizer. To test the ^{2}H lock unit, the variation in B_0 was monitored by the frequency offset in the ^{23}Na resonance line of an aqueous $NaNO_3$ sample. The inlet water temperature was regulated in ''manual'' mode with a tolerance of 0.3°C. Under these conditions and without the lock, an 8.5 ppm variation in the ^{23}Na frequency was observed as demonstrated in Fig. 3. Stability is improved by nearly an order of magnitude (to 0.9 ppm) when the field is locked. Hence, we can maintain 1 ppm temporal stability when the variation of the inlet water temperature does not exceed 0.3°C. At the present time, the field/frequency lock does not maintain a locked condition when the variation in the magnetic field is too large and too sudden, such as when another resistive magnet ramps, causing a 3 to 4°C change in the inlet water temperature. This results in a frequency shift of 50 to 70 ppm and loss of the locked field. Our solution to this particular problem is twofold: locally at the magnet, a fast response thermoelement at the inlet water pipe is being installed to detect variations in the inlet temperature and to maintain it to within 0.3°C. The second complementary approach is to modify the control system, from a temperature-regulation control scheme to flow-based control.

The variation in the ^{2}H resonance offset frequency over a 25 mm distance along the Z axis of the magnet is 46 ppm. The variation in frequency within a cylindrical volume defined by the 25 mm height and 10 mm diameter is 123 ppm. Within this volume, regions of higher homogeneity have been identified, and shim corrections will be made to optimize the spatial homogeneity over a 10 mm diameter of spherical volume.

Within the present spatial and temporal restrictions, a number of deuterium powder pattern spectra and spectra of uniformly oriented samples have been recorded. These

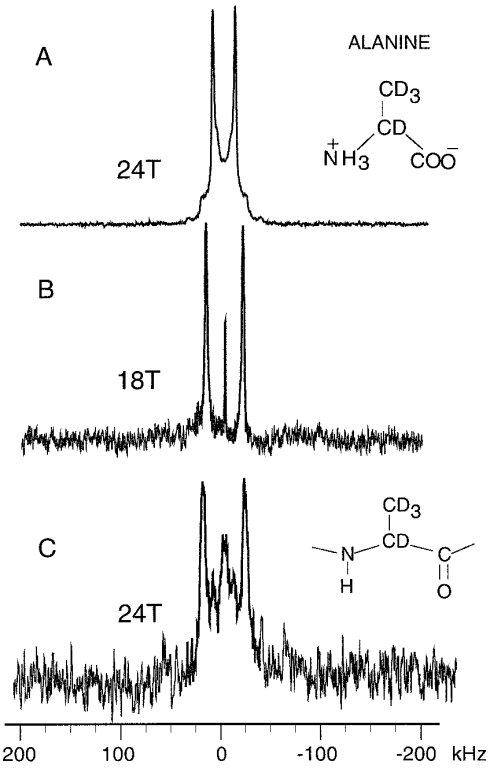

FIG. 4. ^{2}H spectra of d_4-alanine in which the spectra are dominated by the methyl resonances. (A) A 24.6 T powder pattern spectrum of the amino acid obtained with 2.2 μs 90° pulses, 15 μs echo delay from a 2 mg sample with 8 acquisitions. (B) Spectrum of the aligned sample in an 18 T superconducting magnet using $6 \times 7 \times 8$ mm sample volume, 5 μs 90° pulses, 15 μs echo delay, and 9624 acquisitions. (C) As in (B) but obtained at 24 T in a resistive magnet with 2048 acquisitions.

preliminary experiments reveal short quadrupole-echo delays (15 μs) that will allow for the detection of signals unobtainable at lower field strengths where echo delays are longer due to the frequency dependence of acoustic ringing. This advantage is exploited for samples in liquid-crystalline media where sensitivity is often compromised by efficient T_{2e} relaxation. The molecule of interest here is linear gramicidin A, a pentadecapeptide that forms a monovalent cation-selective channel in hydrated lipid bilayers. A high-resolution three-dimensional structure has been achieved by solid-state NMR of preparations in aligned DMPC bilayers (*6, 7*). The dynamics and structure of both the backbone and side chains of this dimeric channel structure are of interest in structure–function relationship studies.

Figure 4 compares spectra of d_4-Ala_5-labeled gramicidin A with the d_4-alanine (amino acid) powder sample. All spectra are dominated by the methyl deuterons that undergo rapid rotation about the $C_\alpha - CD_3$ axis. The alanine powder-pattern spectrum in Fig. 4A was obtained with 8 acquisitions on a 2 mg sample using 2.2 μs 90° pulse width and a 15 μs echo delay. In Figs. 4B and 4C, spectra of gramicidin in hydrated bilayers (1:8 molar ratio of peptide to lipid), with the bilayer normal and channel axis aligned parallel to B_0, are depicted. These spectra represent a volume of $6 \times 7 \times 8$ mm, and consequently the 24 T spectrum in Fig. 4C is substantially corrupted by the spatial inhomogeneities described above. Figure 4B shows the spectrum of the same sample obtained in an 18 T superconducting magnetic field with homogeneity better than 1 ppm over the sample volume. The substantially broadened 24 T spectrum was obtained with only 2048 acquisitions while the 18 T spectrum represents 9624 scans. Once the spatial inhomogeneities are corrected in the resistive magnet, a study of sensitivity enhancement as a function of field strength will be conducted.

ACKNOWLEDGMENTS

This interdisciplinary effort would not have been possible without the visionary leadership by H. Schneider-Muntau of the Magnet Science and Technology group at the NHMFL. Within this group, we gratefully acknowledge the computational efforts of Y. Eyssa and the development of the 24.6 T magnet by M. Bird and his group. In addition, support from M. Sabo, R. Verraneault, and B. Dalton of the control room staff and P. Murphy and A. Powell of the electronic shop were very much appreciated. T.A.C. also acknowledges financial support for this work from the NHMFL and NSF (MCB-9317111).

REFERENCES

1. M. D. Bird, S. Bole, Y. M. Eyssa, B-J. Gao, and H-J. Schneider-Muntau, *IEEE Trans. Magn.* **32,** 2542 (1996).
2. T. A. Cross, G. Drobny, and J. Trewhella, ''Stable Isotope Applications in Biomolecular Structure and Mechanisms,'' (J. Trewhella, T. A. Cross, and C. J. Unkefer, Eds.), p. 315, Los Alamos National Laboratory Press, Los Alamos, New Mexico, 1994.
3. J. M. Koons, E. Huges, H. M. Cho, and P. D. Ellis, *J. Magn. Reson. A* **114,** 12 (1994).
4. T. Meersmann, M. Schwager, V. Varma, and G. Bodenhausen, *J. Magn. Reson. A* **119,** 275 (1996).
5. P. L. Kuhns, A. Kleinhammes, W. G. Moulton, and N. S. Sullivan, *J. Magn. Reson. A* **115,** 270 (1995).
6. R. R. Ketchem, W. Hu, and T. A. Cross, *Science* **261,** 1457 (1993).
7. R. R. Ketchem, K.-C. Lee, S. Huo, and T. A. Cross, *J. Biomol. NMR* **8,** 1 (1996).